ESTIMATION AND ANALYSIS OF TOTAL SUSPENDED SOLID YIELDS FROM THE MICA CREEK EXPERIMENTAL WATERSHED, IDAHO

A THESIS

SUBMITTED TO THE FACULTY OF THE UNIVERSITY OF MINNESOTA

BY

Charlie Elverson

IN PARTIAL FULFILLMENT OF THE REQUIREMENTS

FOR THE DEGREE OF

MASTER OF SCIENCE

Diana L. Karwan

August 2016

© 2016 Charlie Elverson

All Rights Reserved

ACKNOWLEDGEMENTS

I would like to extend my thanks to my advisor, Dr. Diana Karwan for her support. I would also like to thank my committee members, Dr. Bruce Wilson and Dr. Matthew Russell for their input and guidance throughout the research process.

This project was made possible by data contributions from the Potlatch Corporation and John Gravelle and the financial support of the Department of Forest Resources and Peter F. Ffolliott fellowship.

Finally, I cannot thank my wife, Dr. Jessie Ingvalson, enough for her support throughout the last two years. Despite her grueling schedule, Jessie was always there to help when I needed it.

Abstract

Transport and concentration of Total Suspended Solids (TSS) in forested streams play an important role in ecosystem health, affecting the health of fish populations and playing a role in nutrient delivery to floodplains. Despite a long history of studying TSS yields, estimates of TSS yields remain uncertain. Multiple methods have been commonly used to estimate time-aggregated TSS yields from water samples. This study investigated the effects of contemporary timber harvest practices on TSS yields as well as the robustness of conclusions to different methods of TSS yield calculation. TSS yields were calculated using linear interpolation, flow-weighted averaging, and statistical regression. The study utilized a paired-watershed design, with 6 years of calibration data between the control watershed and 2 treatment watersheds. One watershed was clearcut across 50% of its area and allowed to recover for the remaining 12 years of the study period. The other treatment watershed had 50% of basal area removed across 50% of it's total area. After the thinning treatment, the watershed was allowed to recover for 9 years before being clearcut across 46% of the area which was originally thinned. The watershed was then allowed to recover for the remaining 3 years of the study. Harvest impacts on TSS yield varied between treatment watershed and season, with the most significant changes occurring during spring (March through June). Furthermore, the different methods of TSS yield estimation provided different conclusions about TSS yield trends as well as total yields, with statistical regression providing the most consistently defensible estimates.

Table of Contents

List of Tables

List of Figures

Introduction

Forest Management and Water Quality Concerns

Transport of sediment and other solids through watersheds is a key process in ecosystem functioning, providing both substrate and nutrients to downstream ecosystems. However, in excess, suspended solids, sediment, and the resulting turbidity cause a myriad of water quality and stream ecosystem health concerns. Sediment and related concerns remain a top water quality issue in managed forest systems [*Bilotta and Brazier*, 2008]. In forested systems, such as Mica Creek Experimental Watershed (MCEW), suspended solids are high in organic content, forming flocs and aggregates. These particles are comprised of inorganic sediment bound with organic components, such as bacteria and the products of microbial respiration [*Droppo*, 2001; *Droppo et al.*, 2005]. In excess, biological breakdown of these particles has the potential to deplete dissolved oxygen needed by fish [*Ryan*, 1991; *Bilotta and Brazier*, 2008]. Therefore, understanding TSS transport is essential to understanding ecosystem functioning, especially under changing conditions.

Previous studies have linked increased TSS yield with forest management practices [*Megahan et al.*, 1995; *Karwan et al.*, 2007]. Research on broad trends in forested catchments has not revealed an obvious relationship between proportion of watershed area harvested and a change in sediment yield [*Bathurst and Iroume*, 2014]. This suggests that sediment yield is more strongly influenced by other factors, such as location within the watershed, method of harvest, and the connectivity of the harvested

area to stream networks. There is considerable evidence for this relationship, with regard to other water quality parameters, such as dissolved oxygen, temperature, and invertebrate community composition [*Baillie et al.*, 2005].

Management concerns over suspended sediment can broadly be categorized by the issue and timeframe of concern: concentration (often measured as Total Suspended Solids in mass per volume of water) or yield (the total mass of solids per unit time). Although many managers may be concerned with only one of these quantities, concentration and yield are mathematically related, as yield is the product of concentration and stream discharge integrated over a given time interval (e.g. month or year). When assessing fish habitat, TSS concentration is likely to be the primary concern. Previous studies have linked suspended sediment concentration with negative effects on salmonid fish, such as trout, due to clogging and abrasion of gill structures [*Bilotta and Brazier*, 2008]. Increased suspended solids concentration have also been linked to increased risk of infection, higher stress levels, and lower feeding rates in salmonids [*Redding et al.*, 1987; *Greer et al.*, 2015]. Elevated turbidity levels, often associated with increased TSS concentrations, have been linked with reduced foraging success and gill deformation in juvenile snapper (*Pagrus auratus*) [*Lowe et al.*, 2015]. However, for reservoir management, TSS yield is more important. If stream discharge increases, but TSS concentration remains constant, sensitive species may be largely unaffected because TSS concentration has not been altered. However, the manager of a reservoir may be concerned, as sediment will deposit at a higher rate, requiring more frequent dredging or flushing.

Although excess suspended solids can be detrimental, insufficient supplies can be problematic, as well. Sediments from upstream supply soil to floodplains, mud flats, and deltas. In multiple locations around the world, such as the Ebro delta of Spain and Nile delta of Egypt, inadequate sediment supply has resulted in major river channel incision [*Owens et al.*, 2005; *Vericat and Batalla*, 2006] and can lead to the loss of these important habitats. The suspended solids from forested catchments play an important role in riparian systems by supplying not only sediment but also organic material. In addition to providing substrate, in the form of sediment, to downstream habitats, flocs and aggregates are a potential food source for a variety of benthic suspension and filter feeders [*Wotton*, 2007]

Current methods of data analysis

Historically, stream water quality studies have collected near continuous discharge measurements and paired them with less frequent water quality samples, to measure constituent concentrations. Once a time series of water quality samples has been collected and chemically analyzed, their data is assembled. However, this is point data, which is not temporally continuous. A variety of methods, such as linear interpolation, flow-weighting, transport or rating curves, and statistical regression, have been used to make this data temporally continuous in order to compute a time-integrated yield or load [*Smart et al.*, 1999; *Coats et al.*, 2002; *Runkel et al.*, 2004; *Benaman and Shoemaker*, 2005; *Quilbé et al.*, 2006; *Karwan et al.*, 2007; *Gray and Simões*, 2008; *Raymond et al.*, 2014; *Appling et al.*, 2015]. Linear interpolation assumes that concentration changes linearly between adjacent measurements to estimate concentrations for time steps

between observations. This method makes intuitive sense, especially with closely spaced observations, and has a long history of use [*Benaman and Shoemaker*, 2005; *Karwan et al.*, 2007; *Gray and Simões*, 2008]. Flow-weighting estimates the average concentration in a given time interval as a weighted mean of measured concentration values, with instantaneous stream discharge as the weighting factor. Implicit in this method is the assumption that higher stream flows make up more of the total water yield. The rating curve method uses measured data to fit a curve to stream discharge and concentration (or load) data. The curve is generally fit to the log-transformations of these data. Using the log-transformations results in a power law relationship between concentration and discharge [*Gray and Simões*, 2008]. Rating curves are a special case of statistical regression[*Runkel et al.*, 2004]. Statistical regression can use multiple input parameters, such as antecedent stream discharge, time of year, and polynomials, to estimate concentration, and is widely supported in the literature. For example, freely available statistical packages, such as Loadflex and EGRET, were recently developed to facilitate load estimation through multiple methods [*Hirsch and De Cicco*, 2014; *Appling et al.*, 2015]. The USGS package LOADEST uses a statistical regression framework to estimate yields [*Runkel et al.*, 2004]. In both the rating curve and statistical regression methods, the calibrated relationship is used to estimate concentration for each time step. Previous works have explored multiple estimation methods and shown thatthe method used to estimated loads can have significant impacts on the estimates, in terms of both mean and bias [*Smart et al.*, 1999; *Coats et al.*, 2002]. We take this analysis one step further and ask

how load estimation method affects our conclusions about the hydrologic effects of landscape change.

We quantify the effects of timber harvest on the TSS yield of 3 small watersheds in northern Idaho with specific attention to the influence of our chosen methods of estimation on our conclusions about the hydrologic effect of timber harvesting While ultimately interested in sediment yield, we also examine changes in water yield .

This study has two null hypotheses: (1) timber harvest treatments within MCEW do not have a measurable effect on TSS yields and (2) the conclusions from hypothesis 1 are not dependent on the method used to estimate TSS yields. Despite a long history of study, accurate estimation of sediment yields continues to confound research. In this research, we seek to help managers and researchers what methods are appropriate for their purposes.

Methods

Study Site

The Mica Creek Experimental Watershed (MCEW) consists of 7 nested and paired watersheds in northern Idaho. For the purposes of this study, 3 paired second-order watersheds were considered (Figure 1). These watersheds range in elevation between 1170 and 1600 m above mean sea level. Average annual air temperature is 5 °C and average annual precipitation is 1500 mm, with approximately 1000 mm falling as snow. The soils are characterized by silt loam with gneiss and quartzite parent materials

[*Gravelle et al.*, 2009]. The hillslopes range from 15 to 30% gradients with stream gradients from 3 to 14% [*Gravelle et al.*, 2009].

The hydrology of the watersheds is consistent with typical snow-dominated systems. During winter, November through February (NDJF), stream discharge is typically at or below 14 L s^{-1}, and snow accumulates into a seasonal snowpack, with rare melting and/or rain-on-snow events. Sample lines occasionally freeze during winter, temporarily stopping sampling. During the spring snow-melt season (March through June, or MAMJ), stream discharges are frequently sustained at 140 L s^{-1} and can exceed 280 L s^{-1}. Increased discharge can last for a week or more and watersheds typically show increased flows in unison. The rate of snow-melt is the primary driver of stream discharge, with occasional and are rain-on-snow events also contributing to flow.

During the summer season (July through October, or JASO), typical baseflow is approximately 14 L s^{-1}, with flows increasing up to 10-fold (57-140 L s^{-1}) during occasional thunderstorms. The most extreme summer storm during our period of record generated a discharge of 280 L s^{-1}. Summer thunderstorms are often highly localized in time and space and may affect all or only a subset of our study watersheds. Indeed, multiple times throughout the data record, only one or two of the studied watersheds experienced storm discharge, during a given time period. Increased discharge from summer storms averaged 21.5 hours with a median of 9.5 hours. These hydrologic characteristics and the timing of snow-melt and accumulation were used to break years into 3 seasons: winter / snow accumulation (NDJF), spring / snow melt (MAMJ), and summer (JASO).

The watersheds considered here, watersheds 1, 2, and 3 (abbreviated WS1, WS2, and WS3) are, respectively, 1.4, 1.77, and 2.27 km^2. These 3 watersheds comprise a classic paired watershed design [*Loftis et al.*, 2001]. WS3 was maintained as the control watershed for treatments in WS1 and WS2 (Figure 1).Vegetation, at the start of the study period, consisted of 65 to 75 year-old naturally regenerated conifers, with the canopy composed of dense stands of grand fir (*Abies grandis*), Douglas-fir (*Pseudotsuga menziesii*), western redcedar (*Thuja plicata*), and western larch (*Larix occidentalis*) composing the major species [*Karwan et al.*, 2007]. Previous to this study, the site was last harvested during the 1920s and 1930s [*Hubbart et al.*, 2007].

Limited road construction was performed in 1990, for installation and maintenance of flumes. This road had no stream crossings and was built to minimize hydrologic effects. Effects of this road, if any, are accounted for during the subsequent calibration period (described below). In September 1997, roads were improved and constructed in order to facilitate improvements and construction were done to enable commercial timber harvest. The existing Blackwell Hump road, which passes through the 3 watersheds considered here, was graded, widened, and had trees and brush removed from the road cut. This included a necessary stream crossing in the control watershed (WS3). Within the WS3, particular efforts were taken to minimize the hydrological effect of this single crossing. The Blackwell Hump road (Figure 1) contains the only road-stream crossing in watershed 3. Because this watershed was intended as the control for treatments on watersheds 1 and 2, efforts were made to minimize the crossing's impacts. The road was covered in rock for 30.5 m on either side of the crossing, water control

structures were built to divert water off the road, and straw bales were placed near the road-stream crossing to trap sediment.

The initial timber harvests in this experiment occurred in 2001, when WS1 was clearcut across 47% of its area. After the clearcut, WS1 was burned and replanted in the last week of May 2003. Watershed 2 had 50% of basal area removed across 54% of its area, with the final 10% of log hauling and processing occurring in early summer of 2002. In 2010, WS2 was clearcut across 52% of the initially thinned area (resulting in 28% of the watershed area being clearcut).

In order to investigate the affects of harvest on the treatment watersheds, the study period was broken into intervals corresponding to the timing of treatments Table 1. Due to the different number of treatments, WS1 and WS2 interval definitions differed in the latter half of the study. Previous studies at MCEW found the significant effects of treatment on sediment yields were constrained to the first year after treatment [*Karwan et al.*, 2007]. Therefore, the year following any treatment was always separated into its own interval. After the first year, the subsequent period is referred to as a recovery interval. In WS1, the period after the clearcut is divided into 3 intervals. First, is the immediate post-harvest interval, for the year following harvest. Then, there is a recovery interval which lasts from 2002 to 2008. The period after 2008 is termed extended recovery. The reason for this distinction is to isolate the differences between early recovery of the watershed, when it was burned and replanted and the later period when new tree growth had occurred. The transition from recovery to extended recovery was placed in 2008 to give each interval similar numbers of seasons for analysis. Furthermore, as WS1 and WS2

yields are not compared, coordinating the timing of their treatment intervals was not prioritized. In WS2, no such extended recovery interval was used, as the watershed was harvested again in 2010. Harvest intervals are summarized in Table 1.

Timber harvest followed Idaho Forest Practice act guidelines, with stream protection zones along fish-bearing streams and smaller equipment exclusion zones along non-fish-bearing streams. Line skidding was used in areas with greater than 20% slopes and tractor skidding was used for lower-angled slopes. Water routing structures were constructed on all skid trails after the harvest period.

Data Collection

Beginning in 1991, stream discharge was measured every 30 minutes using steel Parshall flumes and nitrogen bubbler pressure transducers accurate to ±3 mm (Riverside Technology Inc., Fort Collins, CO). TSS samples were collected at variable time intervals using ISCO 3700 automatic samplers and subsequently analyzed for Total Suspended Solids (TSS) by EPA Method ###. Samples were collected when one of 2 criteria were met: (1) cumulative stream discharge since the last TSS sample or (2) stream stage increased by a threshold amount in the preceding 30 minute interval [*Karwan et al.*, 2007]. This sampling protocol was chosen to sample both storm and baseflows at a remote field site. Daily precipitation, including snow and snow-water equivalent (SWE) was measured at the Mica Creek SNOTEL station, approximately 2 km southeast of WS1 (Figure 1). Daily SWE measurements were used to categorize days as melt or non-melt.

Data Analysis

Statistical analysis was carried out on a seasonal basis (i.e. JASO and MAMJ yields are considered separately) in order to evaluate watershed response to landscape change in our snow-melt driven system [*Hubbart et al.*, 2007; *Karwan et al.*, 2007; *Kumar et al.*, 2013; *Appling et al.*, 2015]. NDJF yields were not analyzed individually, due to the prevalence of snow accumulation during this season, as indicated by the relatively small contribution these months have to the annual water yield and low number of TSS samples during this interval (Table 6). Monthly yields were chosen as the base unit for analysis because smaller units of time did not consistently contain enough data to create estimates of yield. Using the smallest time step feasible with the data set provides the option of detailed analysis, such as the timing of yields within a given season. Seasons were considered independently of each other because of the significant difference in hydrologic drivers and magnitude of water yields in different parts of the year.

Water and TSS yields were both assessed by analysis of covariance (ANCOVA) through linear regression of monthly yields. Generalized linear models were produced using the R statistical package [R Core Team, 2015], to compare each of WS1 and WS2 yields against WS3 yields using treatment interval as a categorical predictor. Linear regression was performed according to equation 1,

$$Yield_{treatment} = \beta_C + \beta_T + (\alpha_C + \alpha_T) * Yield_{control} \quad (1)$$

where $Yield_{treatment}$ and $Yield_{control}$ are the respective watershed monthly yields (L and kg km^{-2} for water and TSS yields, respectively). Subscripts of C and T, respectively, indicate a parameter for the calibration interval and the offset for each treatment interval. Treatment intervals are defined in Table 1. The β terms represent the y-intercept, and α terms represent the relationship between treatment and control watershed, referred to as yield slope. The significance of α_T, determined by partial t-test, was used to determine if there was a significant change in relationship between the yield from the control watershed and treated watershed during each time interval. A non-zero α_T was taken to indicate a change in this relationship as a result of treatment [*Loftis et al.*, 2001]. Treatment intervals were considered to have significant change if the associated α_T was significant at the P = 0.1 level. The results of the linear regression models are presented in Table 5, and cumulative yields are presented in Figure 4. Additionally, mean MAMJ and JASO yields were calculated for all intervals to estimate the cumulative effects of treatment on whole seasons. Comparing yields in these two ways provides an estimate of total seasonal change, changes in treatment and control relationships, and whether or not changes were statistically significant.

Previous studies have assumed constant slopes between treatment and control watersheds (i.e. $\alpha_T = 0$) [*Hubbart et al.*, 2007]. With this interpretation of paired-watershed studies, all treatment effects are assumed to be seen as a constant change in yield, as a result of treatment, represented by a change in model intercept. Thus, the treatment effect is assumed to be the same throughout a treatment interval, regardless of hydrologic condition. However, previous research has indicated that, when it comes to

water yield, larger changes are observed in wetter years [MacDonald and Stednick, 2003]. This observation is consistent with an interpretation of paired watershed designs, where a change in slope indicates treatment effect. An advantage of comparing intercepts is a change in intercept can be interpreted to mean a constant increase in millimeters of water or kilograms of suspended solids (TSS). Slopes, on the other hand, do not provide a simple physical quantity for interpretation. Instead, a change in slope indicates a change which is proportional to the hydrologic inputs, such as precipitation and snowmelt, or the rate at which treatment yield can be expected to increase per unit increase in control yield.

TSS and water yields were calculated on a monthly basis. Water yields were calculated by summation of measured discharge values over the entire month, assuming constant discharge over the 30-minute measurement interval. . TSS yields were calculated using 3 methods: (1) linear interpolation, (2) flow-weighting, and (3) statistical regression. Linear interpolation estimates of TSS (mg L^{-1}) were calculated by standard interpolation methods and applied to the time of each discharge measurement when a water sample was not collected [*Gray and Simões*, 2008]. To calculate monthly yields from this, the measurements of discharge and estimates of TSS, at each point, were multiplied together, assumed constant over the 30-minute measurement interval, and summed for the given month. Flow-weighted estimates were calculated by multiplying the flow-weighted average TSS concentration with monthly water yield. The monthly flow-weighted average was calculated by equation 2,

$$[TSS] = \frac{\sum Q_i * C_i}{\sum Q_i} \quad (2)$$

where C_i is the i^{th} measurement of TSS concentration during the month of interest and Q_i is the corresponding measurement of discharge [*Smart et al.*, 1999]. A visual illustration of the flow-weighting and linear interpolation methods is provided in Figure 2. To compare the yield estimates for each method, Tukey's honest significant difference (HSD) test was applied to seasonal yields calculated by each method within, at each watershed. Tukey's HSD test estimates the average difference between estimates from each method and gives a probability that the difference is statistically significant. Sensitivity analysis was also performed, for 2 months of data, to compare the resilience of each method to variations in TSS sample concentration. April 2012 and October 1995 were chosen for sensitivity analysis, as they represent the average month for their respective seasons with respect to number of TSS samples and stream discharge. Sensitivity analysis was performed by generating randomized TSS samples at each time step for which a real TSS sample was taken. This randomized sample was drawn from a normal distribution with a mean matching the measured sample and standard deviation of 10% of the measured sample. These randomized data records were used to calculate new monthly yield estimates for each of the 2 months.

Statistical Regression Development

In flow-weighting, linear interpolation, and statistical regression (described next), the instantaneous TSS yield is computed as the product of estimated concentration and

measured stream discharge. The monthly yield is then computed by integrating this product over the month and assuming a constant yield over the 30-minute discharge measurement interval. The statistical regression method presented here follows a similar framework as the LOADEST package by USGS [*Runkel et al.*, 2004]. Statistical regression can be broken down into 3 steps: (1) model parameterization, (2) model fitting, and (3) model application. Model parameterization is the process of selecting predictors and creating the model equation. Data from WS3 (the control) was used to develop the parameterizations. After parameterization, the model was fit to each watershed. Fitting is the process of adjusting the coefficients, β terms in the following equations, to best fit the data. Fitting the model to each watershed independently is important because although the watersheds may respond to the same drivers, their responses are not likely to be identical due to differences in physical characteristics, such as size, slope, and hydrologic connectivity. Finally, the models are applied at each watershed to estimate TSS concentrations at each time step. To adequately represent the watersheds, 3 models were implemented. Model selection was performed using the Akaike information criterion (AIC).

MAMJ and NDJF were modeled with the same relationship, fitted separately to each season. TSS concentrations were modeled, at each time step, using the relationship in equation 3,

$$TSS = F\left(Q, Q_{rel}, Q_{rel}^{2}, melt\right) = \beta_1 * Q + \beta_2 * Q_{rel} + \beta_3 * Q_{rel}^{2} + \beta_4 * Q_{rel} * Q + \beta_5 * Q_{rel}^{2} * Q + \beta_6 \qquad (3)$$

where TSS is concentration in mg L^{-1}, Q is current discharge [L s^{-1}], Q_{rel} is relative discharge [L s^{-1}] (the difference between current discharge and minimum discharge in the preceding 12 hours). Q^2_{rel} is an orthogonal polynomial of Q_{rel} [*Narula*, 1979]$_l$. Melt is a categorical variable defining whether snow is melting, not melting, or not present, based on daily SWE measurements from the Mica Creek SNOTEL site. The coefficients, β_i, were estimated independently for each watershed and melt status. Model fitting was performed using least-squares and evaluated by the glm() function in R.

JASO was modeled in 2 ways, depending on hydrologic condition (baseflow or stormflow). No suitable relationship was found to represent TSS concentrations during baseflow. Despite a variety of model parameterizations, involving Q, Q_{rel}, parameters from the JASO storm regression, and even running models on subsets of the data based on measured TSS concentration, the highest adjusted R^2 was under 0.03, with one exception. When baseflow measurements were restricted to TSS concentrations greater than 25 mg L^{-1}, a restriction which is unreasonable to apply for modeling TSS concentration, and returned only 14 measurements, adjusted R^2 was 0.37. Therefore, median observed TSS concentration, during baseflow, for each watershed, was used. Median was chosen over mean, as the distribution of baseflow TSS concentrations was skewed by a handful of high TSS concentrations. During stormflows, a regression based on discharge parameters was used After storms were identified (described below), regressions were fit to each watershed during stormflows. JASO stormflow TSS concentrations were modeled using the relationship in equation 4,

$$TSS = F(Q_{rel}, Q_{rel}^2, Q_{L1R}) = \beta_1 * Q_{rel} + \beta_2 * Q_{rel}^2 + \beta_3 * Q_{L1R} + \beta_4 * Q_{rel} * Q_{L1R} + \beta_5 * Q_{rel}^2 * Q \quad (4)$$

where Q_{L1R} is Q_{rel} from the preceding time step and Q_{rel} and Q^2_{rel} are the same as the equivalent terms in equation 3.

In order to identify JASO stormflows, the measurements of stream discharge were compared sequentially. At each time step, 2 windows of time were identified: a test window was defined, in which the algorithm looked for evidence of stormflow. For WS1 and WS2, the test window was 4 hours and for WS3 it was 6 hours. A base window, defined as the most recent 24-hour period for which no storm was detected was also defined for comparison with the test window, in order to capture the range of diurnal fluctuations in baseflow. Starting at the beginning of the data record, if the minimum discharge in the test window exceeded the maximum discharge in the base window, the test window was designated as a storm. The storm was then ended at the first subsequent measurement, which fell below the maximum value of the base window. With base and test windows sized to our watersheds, this method reliably identified summer stormflows in the small watersheds of MCEW and had multiple advantages over manual identification or using hyetographs to delineate storms. Prior to the early 2000's, only daily measurements of rainfall were available, which could not provide the level of detail needed to define stormflows on less than a daily time-step. Furthermore, there were many summer stormflows, throughout the study period, which had no measured rainfall at the SNOTEL site, presumably due to the highly localized nature of summer storms. It's also possible the minimum measurement threshold of the SNOTEL precipitation collector (0.1

inches) was not met during individual storms which still produced stormflow. Finally, manual identification, based solely on hydrographs, is subject to individual interpretation, whereas this method provides a consistent basis for storm identification and is easily adapted to similar watersheds for future use.

Results

Water Yield

Although this research is targeted at assessing changes in TSS yield, water yield analysis was necessary as well, to help understand the drivers of any changes in TSS yield. Each flume produced approximately 400,000 measurements of stream discharge during the study period. Mean seasonal water yields are summarized in Table 2 and Table 3. Average water yield, during MAMJ, in the calibration interval was 391 mm in WS3 and 373 mm in WS2 (Figure 3a, Table 2). During the recovery intervals, following thinning and clearcut (intervals 5 and 7), average MAMJ water yields from WS2 were 93 mm and 209 mm higher than WS3, respectively. In these same intervals, WS3 water yield averaged 361 and 459 mm, respectively. In the year immediately following thinning and clearcut (intervals 4 and 6), MAMJ water yields from WS2 were 71 mm and 116 mm higher than WS3, which averaged 499 and 843 mm, respectively. In MAMJ, significant increases in WS2 water yield slope were detected during the immediate thinning, thinning recovery, and clearcut recovery intervals (intervals 4, 5, and 7). The only post-harvest interval which does not show statistically significant change is the year immediately following the clearcut (interval 6) (Table 5). No significant changes were detected as a

result of road construction (intervals 2 and 3). During JASO, WS2 showed no significant changes in water yield slope (Table 5).

During calibration, average MAMJ water yield at WS1 was 7 mm less than that of WS3, where average water yield was 391 mm (Table 4, Figure 3c). In the year immediately following clearcut, MAMJ water yield was 216 mm higher in WS1 than WS3, which had a water yield of 499 mm. During the recovery and extended recovery periods, average MAMJ water yields from WS1 were 181 mm and 113 mm higher than WS3, where water yields averaged 346 and 515 mm. During JASO, average water yields from WS1 were higher than those of WS3 for all treatment intervals, except the extended recovery (Figure 3d). During the extended recover interval, average JASO water yields from WS1 are 20 mm lower than WS3. In MAMJ, WS1 showed significant increases in water yield slope for all intervals following harvest (Table 5). The highest rate was immediately after clearcut, with less increase during the recovery period, and the lowest increase during extended recovery. In JASO, WS1 showed a significant decrease in water yield slope during the clearcut recovery period.

Total Suspended Solids

Measured TSS concentrations ranged from 0 to 993 mg L^{-1}, with the highest concentration recorded in May 1998 at WS1. Overall, 95% of measured TSS concentrations were below 35 mg L^{-1}. WS1, WS2, and WS3 had 2503, 2003, and 1895 total TSS measurements, respectively during the study period. The watersheds, respectively, had 100, 124, and 106 TSS observations during JASO stormflows, and

1646, 1283, and 1313 measurements during MAMJ. Overall, 15.6% of JASO TSS samples during were taken during stormflows, but 6.8% of the time in JASO was stormflow. TSS measurements are summarized by season and watershed in Table 6. MAMJ months consistently contained multiple TSS samples per week and sometimes multiple per day, with an overall average of 16.3 per month. During JASO, multiple months contained no TSS samples and the overall average was 6.2 samples per month.

TSS Yields

The mean and 95th percentiles of monthly TSS yield for each watershed, by season and method are summarized in Table 7. Mean seasonal yields are summarized by treatment interval and estimation method in Table 2, Table 3, Figure 5, and Figure 6. The results of Tukey's HSD test on seasonal yields are presented in Table 6. There are no significant differences in yields estimates during MAMJ. During JASO, all watersheds show significant differences between estimates of yield from flow-weighting and statistical regression. During JASO, Statistical regression consistently estimates the lowest yields and flow-weighting estimates the highest yields.

Average monthly statistical regression estimates, during JASO, range from 69 to 141 kg km^{-2}. For the same months, average linear interpolation and flow-weighting estimates range from 135 to 208 kg km^{-2} and 196 to 361 kg km^{-2}, respectively. For all methods, during both MAMJ and JASO, the average monthly yield estimates are lowest in WS3. During MAMJ, the lowest yields are estimated by linear interpolation and the highest are calculated by flow-weighting. During MAMJ, average yield estimates by

linear interpolation, flow-weighting, and statistical regression are 597 to 1117 kg km^{-2}, 901 to 1661 kg km^{-2}, and 810 to 1202 kg km^{-2}, respectively. In WS3, during MAMJ and JASO, flow-weighting estimates averaged 7% and 175% higher than statistical regression estimates, respectively, and linear interpolation averages 13% lower during MAMJ and 127% higher during JASO, compared to statistical regression. Cumulative TSS yield double-mass plots for each treatment watershed and method are presented in Figure 4. Sensitivity analysis showed proportionally lower variation in yield estimates from all methods, for April 2012, compared to October 1995. Both months showed the greatest variation in estimates from Flow-weighting and the least variation from statistical regression (Table 8).

Flow-Weighting

During MAMJ, in WS2, flow-weighting shows a significant decrease in TSS yield slope during the period immediately after road construction (Table 5). During JASO, there are no intervals with a significant change in sediment yield slope. However, although not statistically significant, the period immediately after the clearcut indicates a negative relationship between the control and treatment watersheds. Using flow-weighted TSS yields, during MAMJ, there are no significant changes in the sediment yield slopes of WS1. However, during JASO, the road recovery and extended recovery intervals show significant decreases in sediment yield slopes (Table 5). During MAMJ, WS1 shows the highest TSS yield in the periods immediately following road construction and clearcutting. Consistent with the linear models, these increases diminish with time since the harvest (Table 5). The period immediately following clearcut shows an increase in

MAMJ TSS yield from WS1, with 255% (10553.5 kg km^{-2}) of the yield of WS3, as compared to an average of 124% (4191.5 kg km^{-2}) of the WS3 yield during calibration. There is a smaller difference in relative yields in the clearcut recovery interval with WS1 yield calculated to be 223% (6776.5 kg km^{-2}) of the WS3 yield, and by the extended recovery interval, WS1 yield is 159% (6194.9 kg km^{-2}) of the WS3 yield.

Linear Interpolation

During both MAMJ and JASO, linear interpolation shows no significant changes in the sediment yield slope of WS2 (Table 5). In WS1, during MAMJ, the period immediately following clearcut shows a significant increase in sediment yield slope. During JASO, there are no intervals which show significant changes in sediment yield slope. During MAMJ, WS1 consistently has higher estimates of TSS yield than WS3. In MAMJ, during calibration, WS1 TSS yields average 141% (3413 kg km^{-2}) of WS3 yields. Immediately after the clearcut, WS1 TSS yield in MAMJ is calculated to be 325% (10127.6 kg km^{-2}) of WS3 yield (Figure 5, Table 2). In the subsequent recovery and extended recovery intervals, average MAMJ TSS yields are 237% (4776.5 kg km^{-2}) and 164% (4897.5 kg km^{-2}) of WS3 yields.

Statistical Regression

The initial statistical regression results gave 3 instances of estimated TSS concentrations greater than 1000 mg L^{-1}. The regression calculated concentrations were 13719, 24449, and 1612 mg L^{-1}. These values were coincident with the largest Q_{rel} value in the data record, at 296 L s^{-1}. In 1 hour, discharge rose from 14 to 311 L s^{-1}, resulting in

Q_{rel} values approximately double what had been seen in the dataset used for model calibration. In the data available for developing the regressions, the highest Q_{rel} value was 151 L s^{-1} and 95% of Q_{rel} values were at or below 36 L s^{-1}. The event which generated these values was a storm in July 1992. In order to deal with these extreme values, the 3 calculated TSS concentrations were lowered to 1000 mg L^{-1}, to approximately match the highest measurement recorded in the 23 years of data collection, 993 mg L^{-1}.

In WS2, during MAMJ, statistical regression shows significant increases in sediment yield slope during periods immediately following harvests (intervals 4 and 6). During JASO, in WS2, there are significant decreases in sediment yield slope during the road recovery, thinning recovery, and immediate post-road intervals (Table 5). During MAMJ, WS2 mean seasonal TSS yields, during calibration, were 110% (3774.7 kg km^{-2}) of WS1 yields. In the post-harvest intervals, WS2 average JASO yields were 142% (7326.7 kg km^{-2}) to 213% (7856.8 kg km^{-2}) of WS3 yields. During JASO, WS2 mean seasonal yields during calibration averaged 228% (462 kg km^{-2}) of WS1 yields. In the intervals with significant drops in yield slope, WS2 average JASO yields were 179% (537 kg km^{-2}) to 243% (434.8 kg km^{-2}) of WS3 yields (Table 4). In WS1, during MAMJ, there is a significant increase in sediment yield slopes during all post-clearcut intervals. During JASO, linear regression indicates lower TSS yield slopes in all post-calibration intervals, in WS1 (Table 5). During MAMJ, statistical regression shows similar average seasonal TSS yields in WS1 and WS3, during the calibration and post-road intervals, with WS1 yields averaging 90% (3092.2 kg km^{-2}) to 120% (2469.4 kg km^{-2}) of WS3 yields. After clearcut, estimated MAMJ TSS yields increase in WS1 to between 177% (9155.1

kg km^{-2}) and 200% (4828.7 kg km^{-2}) of WS3 yields (Table 2). During JASO, in WS1, calibration TSS yields average 203% (411.7 kg km^{-2}) of WS3 yields. Later intervals indicate average seasonal WS1 yields of 90% (393.2 kg km^{-2}) to 168% (299.6 kg km^{-2}) of WS3 yields.

Discussion

Effects of treatment interval and TSS estimation method

Double mass plots illustrate the increases in MAMJ TSS yield slopes from both WS1 and WS2, immediately following harvest activities (Figure 4, Table 5). The intervals which showed statistically significant TSS yield slope increases showed changes similar to those of the water yield slopes. This provides evidence that increases in TSS yields are driven by increased water yields, as opposed to increased erosion rates. During statistical regression parameterization, treatment interval was rejected as a parameter, as it failed to improve AIC scores, providing further evidence that treatments did not have affect TSS concentrations. During JASO, the only significant changes in TSS yield slope were decreases. In JASO, water yield slopes in WS1 and WS2 were lower during post-treatment intervals, but only one clearcut recovery in WS1 showed a statistically significant change.

In WS1, after the clearcut, all methods showed increases in mean TSS yield during MAMJ (Figure 5). The methods did not agree, however, as to which post-harvest interval had the greatest TSS yield slopes or which intervals showed statistically significant changes (Table 5). Both linear interpolation and statistical regression agreed

that the period immediately after clearcut showed the largest increase in TSS yield slope and that the increase was statistically significant. Flow-weighting, however, showed the greatest TSS yield slope, and highest overall seasonal yield, immediately following the road improvements. This result is indicative of flow-weighting's vulnerability to individual outlier measurements. During a high-flow period, TSS concentration was measured at 993 mg L^{-1}. This measurement was concurrent with a large storm peak, and as a result, the flow-weighted mean TSS concentration for the month was 99 mg L^{-1} (Figure 8).

In WS2, during MAMJ, there is also evidence of increased mean seasonal yield after harvest. This can be seen by the double mass plots for statistical regression and linear interpolation as well as the mean yields for the statistical regression. However, flow-weighting and linear interpolation showed an unexpected trend during JASO. Immediately following the 2010 clearcut, these methods indicated a negative trend between WS2 and WS3 TSS yields. This trend is not the result of individual outlier measurements, but it is the result of sparse data during those periods. In September, the linear interpolation and flow-weighting estimates of WS2 TSS concentration were based on 2 storm-associated measurements, whereas measurements in WS3 captured both storm and non-storm periods (Figure 7). The sampling of storms in September led to higher estimates of TSS yield than in August. During that period, the linear interpolation estimate rose by 265 kg km^{-2} and the flow-weighting estimate rose by 308 kg km^{-2}. In contrast, the flow-weighting estimate of WS3 TSS yield was lower in September than August, and the linear interpolation estimate increased by only 15 kg km^{-2}. These months

illustrate the primary short-comings of both linear interpolation and flow-weighting. Slight changes in the timing of measurements can have large impacts on the calculated yield from either method. This is further illustrated by the results of sensitivity analysis (Table 8), where flow-weighting showed the greatest variation in yields, and statistical regression showed the least variation. This issue is of particular concern at MCEW, during JASO, when measurements are infrequent. Even with more frequent measurements, flow-weighting has a second concern. Inherent in the method of flow-weighting is the assumption that instantaneous discharge is the best weighting factor for TSS concentration samples. In order for this assumption to be met, a greater amount of the total water yield must occur during elevated flow conditions. This assumption is not valid during JASO, at MCEW.

Statistical regression is less vulnerable to issues with individual measurements (Table 8), timing of measurements, and sparse data. However, in order to develop a satisfactory statistical regression, data must first be collected which spans the hydrologic conditions seen during the entire study period, and meaningful correlations must be identified. At MCEW, developing these relationships was possible because of the length of sampling and the large data set. At MCEW, and other snow-dominated watersheds, the seasonality of the watershed cannot be ignored. Between seasons, baseflow changes by an order of magnitude and the hydrograph responds to very different drivers. To account for this, seasons were modeled independently of each other in this study. This type of a priori knowledge about a watershed is essential in developing realistic statistical regressions. If such information and a suitable dataset can be obtained, the statistical

regression method can be a powerful tool for more than just yield estimation. Once regressions are developed, they can be used to better understand what drives TSS and other constituent yields and concentrations.

Other statistical approaches were explored, in addition to linear regression. In particular, the more traditional power-law relationship was attempted. Ultimately, non-linear models did not improve model performance. Bootstrap assessments of linear and non-linear models were performed on data from WS3, and split into several bins of measured TSS concentration, in order to assess bias and error across the range of data. Overall, non-linear models failed to outperform the linear models in terms of Root-Mean-Square-Error (RMSE), Mean Absolute Error (MAE) and Mean Bias Error (MBE). At the lowest TSS concentrations, the non-linear models showed slightly better fit, but that was over-shadowed by increasing biases and error at higher TSS concentrations. Additionally, development of non-linear models on this dataset required either removing or systematically modifying a portion of the data record. This was necessary to accommodate the traditional framework used for hydrologic rating curves, which require the logarithmic transformation of the covariate as well as predictors. In this case, TSS concentration was 0 mg L^{-1} in 4% of observations and the relative discharge (Qrel) was 0 L s^{-1} in 12% of observations. TSS concentration and Q_{rel} were both 0 in 0.4% of observations. Thus, developing a power-law based relationship required modifying or ignoring 15% of the observed data. A traditional rating curve, relating log TSS and log discharge was considered but immediately rejected because of poor fit.

TSS Regression Models

The form of the regression equations used to model TSS offers insight into how and when TSS is generated within the watershed. TSS concentration, during both MAMJ and JASO storms is primarily driven by Q_{rel}, with Q and Q_{L1R} dampening the increases in TSS concentration, respectively (Figure 9 and Figure 10). During MAMJ, at low Q levels (<100 L s^{-1}), changing Q_{rel} from 40 to 60 L s^{-1} results in an increase of approximately 20 mg L^{-1} of TSS. However, at Q levels close to 200 L s^{-1}, the same increase in Q_{rel} has negligible impact on TSS concentration. High Q values, concurrent with low Q_{rel} values are indicative of sustained higher levels of discharge. Conversely, high Q_{rel} concurrent with low Q indicates a period of rapid stage increase. This dependence on previous hydrologic conditions indicates that TSS follows a build-up and flushing model, where low-flow conditions allow particles to collect within the stream channel. When stage increase occurs, these particles are quickly flushed down stream. If increased stream stage is maintained, TSS concentration begins to decline as the supply of material is diminished. These observations on the form of the TSS regressions developed here are indicative of clockwise hysteresis loops in concentration-discharge relationships. Such hysteresis loops are well supported in the literature and may indicate the control which organic material has on the amount of suspended sediment in a stream [*Nistor and Church*, 2005; *Underwood et al.*, 2015].

The JASO storm regression is also consistent with this model of TSS generation. However, in JASO, baseflow is consistently below 14 L s^{-1} and shows little variation. This consistency allowed for replacing the Q term in JASO models with Q_{L1R}, a first-

order autoregressive term on relative discharge. By making this replacement, it is possible to differentiate rising and receding limbs of a storm hydrograph. When Q_{L1R} is lower than Q_{rel}, the rising limb of the hydrograph is indicated, and the reverse situation indicates the receding limb. TSS concentrations on the receding limb of the hydrograph are lower than those on the rising limb, as can be seen by the decrease in TSS concentration with constant Q_{rel} and rising Q_{L1R} (Figure 10), providing further evidence of clockwise hysteresis loops in the concentration-discharge relationships at MCEW.

Conclusion

Depending on the method used, one could conclude that there is or is not a significant change in TSS yields after treatments at MCEW. Although the seasonal yields calculated by each method were only significantly different during JASO between statistical regression and flow-weighting (Table 6), the relationships between watershed yields vary considerably. Therefore, it is important to consider the most appropriate method of TSS yield calculation for the dataset considered. When TSS samples are more broadly spaced, flow-weighting and linear interpolation or both prone to over estimating the affects of storm measurements on the monthly yield. Comparisons of watershed yields can also be negatively affected by slight differences in timing of TSS samples between watersheds. This is an issue when WS3 samples a storm and WS1 or WS2 do not sample the same storm flow. This leads to less reliable relationships between watershed pairs. The main shortcoming of statistical regression is whether or not a relationship can be found which accurately represents TSS concentrations across the regime of flow conditions found within each watershed. Statistical regressions applied at MCEW had

adjusted R^2 values which ranged from 0.46 to 0.74, with all but 2 models having values above 0.50.

Given the strength of the statistical regressions at MCEW, and the shortcomings of flow-weighting and linear interpolation, statistical regression should be considered the most reliable method of estimation in these watersheds. The differences between the methods are most evident during JASO, when less frequent measurements make linear interpolation and flow-weighting unreliable. Based on statistical regression estimates of TSS yields, WS2 showed significantly increased MAMJ yield slopes after harvest activity, which were also reflected by increased mean yields. During JASO, WS2 showed significantly decreased yield slopes and little to no change in mean yields. The change in yield slopes without a corresponding change in seasonal yield suggests that the timing of TSS yields changed in WS2. In WS1, the same pattern was observed during both MAMJ and JASO, once again suggesting that TSS yields increased during MAMJ, but only the timing changed during JASO. One difference in WS1 was that in the extended recovery interval (interval 6), all methods indicated lower than expected TSS yields from WS1, as well as decreased yield slopes. This is concluded to be due to decreased water yields, as a result of increased transpiration from the regenerating forest.

Figures and Tables

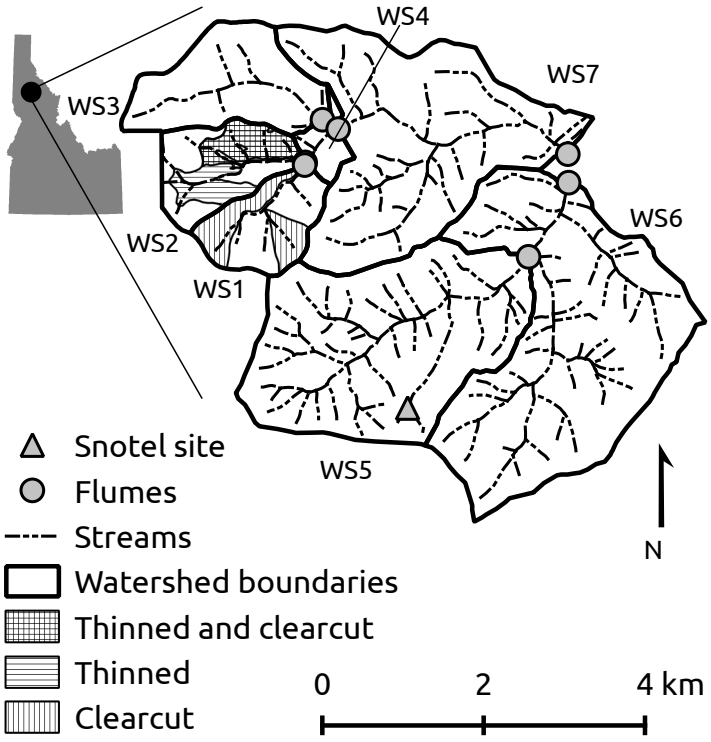

Figure 1 Overview of watersheds at MCEW. Thinning and clearcut were performed in 2001. Clearcut of previously thinned area performed in 2010

Pre-Harvest Intervals			
Interval #	Name	First Month	Last Month
1	Calibration	Apr 1991	Aug 1997
2	Immediate Road	Sep 1997	Jun 1998
3	Road Recovery	Jul 1998	Jun 2001
WS2 Post-Harvest Intervals			
4	Immediate Thinning	Jul 2001	Jun 2002
5	Thinning Recovery	Jul 2002	Jun 2010
6	Immediate Clearcut	Jul 2010	Jun 2011
7	Clearcut Recovery	Jul 2011	Sep 2013
WS1 Post-Harvest Intervals			
4	Immediate Clearcut	Jul 2001	Jun 2002
5	Clearcut Recovery	Jul 2002	Sep 2008
6	Extended Recovery	Oct 2008	Sep 2013

Table 1 Treatment interval names and dates.

Interval	Watershed	Water		Linear Interpolation		Statistical Regression		Flow-Weighting	
		MAMJ	JASO	MAMJ	JASO	MAMJ	JASO	MAMJ	JASO
1	WS3	391.1 (235.2)	61.8 (18.2)	2426.2 (2553.6)	789.4 (383)	3425.1 (3842.9)	202.8 (26.6)	3359 (4300.8)	837.5 (619.2)
	WS1	383.9 (233.4)	72.3 (23.4)	3413 (3299)	1282.9 (1616.2)	3092.2 (3424)	411.7 (280.4)	4191.5 (4441.1)	970.4 (883.8)
2	WS3	323 (*)	62.3 (*)	2083.5 (*)	174.8 (*)	2059.6 (*)	405 (*)	5518.3 (*)	232.7 (*)
	WS1	372.8 (*)	98.9 (*)	6336.6 (*)	370.9 (*)	2469.4 (*)	492.8 (*)	20920.2 (*)	609.9 (*)
3	WS3	384.8 (163)	56.8 (10.2)	1909.1 (770.8)	241.4 (80.8)	3222.5 (1564.1)	178.5 (15.4)	2659.4 (1162.6)	410.6 (370.6)
	WS1	412.2 (185.5)	83 (4.4)	2876.8 (1535.3)	299.7 (84.1)	3192.9 (2002.4)	299.6 (22.3)	3534.4 (2073.8)	415.9 (196.5)
4	WS3	499 (*)	52.8 (*)	3115.1 (*)	174.2 (*)	5163.5 (*)	186.9 (*)	4130.8 (*)	103.7 (*)
	WS1	714.6 (*)	72.1 (*)	10127.6 (*)	604.5 (*)	9155.1 (*)	282.3 (*)	10553.5 (*)	1607 (*)
5	WS3	345.9 (104.2)	74.2 (14.6)	2019.9 (1784.4)	539.4 (314.1)	2409.1 (2043.2)	258.1 (82.6)	3048.5 (3051.4)	1009.7 (1103)
	WS1	526.8 (130.9)	98.1 (11.3)	4776.5 (4775.1)	718.6 (338.5)	4828.7 (4768.6)	367.1 (90.6)	6776.5 (6569.4)	1564.3 (1368.9)
6	WS3	515.1 (227.1)	139 (19.9)	2994.7 (2172)	603.9 (239.8)	3915.3 (2577)	432.1 (62.7)	3893 (3117.7)	596.1 (379.8)
	WS1	628.1 (217.6)	118.7 (17.9)	4897.5 (3065)	447.1 (235.1)	7097.2 (5114.2)	393.2 (63.9)	6194.9 (4492.9)	478.8 (370.1)

Table 2 WS3 and WS1 mean seasonal yields and standard deviations. Water yield in mm. TSS yield in kg km^{-2}.

* indicates only 2 seasons of data were available, therefore standard deviation was not calculated.

Interval	Watershed	Water		Linear Interpolation		Statistical Regression		Flow-Weighting	
		MAMJ	JASO	MAMJ	JASO	MAMJ	JASO	MAMJ	JASO
1	WS3	391.1 (235.2)	61.8 (18.2)	2426.2 (2553.6)	789.4 (383)	3425.1 (3842.9)	202.8 (26.6)	3359 (4300.8)	837.5 (619.2)
	WS2	372.8 (220)	81.2 (20)	4422.2 (5135.1)	646.9 (447)	3774.7 (3949.5)	462 (106.4)	5561.4 (7493.2)	950.4 (971)
2	WS3	323 (*)	62.3 (*)	2083.5 (*)	174.8 (*)	2059.6 (*)	405 (*)	5518.3 (*)	232.7 (*)
	WS2	319.7 (*)	135.6 (*)	2148.4 (*)	306.5 (*)	2155.5 (*)	734.7 (*)	4107.2 (*)	433.7 (*)
3	WS3	384.8 (163)	56.8 (10.2)	1909.1 (770.8)	241.4 (80.8)	3222.5 (1564.1)	178.5 (15.4)	2659.4 (1162.6)	410.6 (370.6)
	WS2	385 (164.4)	101.7 (11.8)	3481.5 (2227.5)	499.4 (277.2)	3368.7 (1618.6)	434.8 (42.3)	4210.7 (2501.6)	983.1 (862.8)
4	WS3	499 (*)	52.8 (*)	3115.1 (*)	174.2 (*)	5163.5 (*)	186.9 (*)	4130.8 (*)	103.7 (*)
	WS2	570.2 (*)	68.2 (*)	6052.4 (*)	572.3 (*)	7326.7 (*)	302.8 (*)	8642.7 (*)	930.6 (*)
5	WS3	361.3 (110.7)	89.7 (31.5)	1919.1 (1599.2)	563.7 (318.7)	2440 (1868.4)	299.7 (104.1)	2839.7 (2713.9)	925 (956.4)
	WS2	453.9 (125.3)	119.5 (37.4)	4074 (2450.7)	1181 (956.4)	4255.1 (2503.3)	537 (183.9)	5007.3 (3360.8)	2044.8 (1809.8)
6	WS3	842.9 (*)	163.4 (*)	4036.2 (*)	649.2 (*)	7129.3 (*)	529.4 (*)	4543.5 (*)	981.5 (*)
	WS2	958.6 (*)	186.9 (*)	4830.4 (*)	970.1 (*)	13999.3 (*)	831.6 (*)	5624.1 (*)	994.1 (*)
7	WS3	458.5 (209.1)	129.6 (26.3)	3852 (3283.3)	548.5 (127.9)	3690.9 (2961.5)	391.3 (50.2)	5247.2 (5019.3)	328.5 (355.8)
	WS2	667.5 (230.4)	185.2 (49.9)	5963.9 (1280.8)	847.4 (287.3)	7856.8 (5779.4)	1058.2 (376.2)	6935.1 (2414.1)	537.8 (222.1)

Table 3 WS3 and WS2 mean seasonal yields and standard deviations. Water yield in mm. TSS yield in kg km^{-2}.

* indicates only 2 seasons of data were available, therefore standard deviation was not calculated.

	WS1			WS2			WS3		
	measurements	mean	95th percentile	measurements	mean	95th percentile	measurements	mean	95th percentile
MAMJ	1646	10.6	35.8	1283	10.9	37.2	1313	7.6	28.4
JASO non-storm	539	5.4	13.4	415	6.3	17.6	332	7.3	14.1
JASO storm	100	38.7	171.6	124	30.2	205	106	14.4	68.3

Table 4 summary of number of measurements and measured TSS concentrations [mg L^{-1}] by watershed, season, and storm status. All seasons and watersheds had a minimum measurement of 0.

		F1				F2			
	Coefficient	**Water**	**LI**	**FW**	**SR**	**Water**	**LI**	**FW**	**SR**
MAMJ	**Calibration Intercept**	1.22 (0.62)	**131.42 (0.06)**	87 (0.23)	30.67 (0.14)	**4.51 (0.02)**	**167.14 (0.04)**	54.41 (0.37)	**55.47 (<.01)**
	Interval 2 Intercept offset	-3.05 (0.79)	-200.8 (0.52)	-7.91 (0.98)	-60.78 (0.46)	8.78 (0.27)	**-207.29 (0.1)**	-8.49 (0.93)	90.24 (0.22)
	Interval 3 Intercept offset	3.8 (0.28)	3.9 (0.97)	22.47 (0.81)	-18.87 (0.45)	**5.95 (0.04)**	-104.39 (0.26)	12.45 (0.87)	35.65 (0.21)
	Interval 4 Intercept offset	10.57 (0.11)	-127.81 (0.15)	-62.18 (0.48)	-18.91 (0.73)	2.52 (0.47)	**-176.24 (0.04)**	-70.02 (0.28)	6.4 (0.87)
	Interval 5 Intercept offset	**13.81 (0.01)**	18.92 (0.86)	106.8 (0.38)	34.13 (0.4)	**11.42 (<.01)**	190.87 (0.15)	**450.83 (<.01)**	**76.51 (0.02)**
	Interval 6 Intercept offset	2.4 (0.69)	**-138.22 (0.09)**	-10.21 (0.92)	21.82 (0.72)	2.93 (0.84)	223.84 (0.45)	328.22 (0.31)	**444.04 (0.07)**
	Interval 7 Intercept offset					**16.67 (0.03)**	123.66 (0.52)	**784.32 (0.05)**	**410.7 (<.01)**
	Calibration Slope	**0.98 (<.01)**	**1.15 (<.01)**	**1.37 (<.01)**	**0.87 (<.01)**	**0.92 (<.01)**	**1.31 (<.01)**	**1.45 (<.01)**	**1.1 (<.01)**
	Interval 2 Slope Offset	0.21 (0.36)	1.95 (0.25)	1.84 (0.27)	0.41 (0.34)	-0.09 (0.53)	-0.22 (0.74)	**-0.81 (0.07)**	-0.34 (0.16)
	Interval 3 Slope Offset	0 (0.98)	-0.12 (0.8)	-0.34 (0.47)	0.04 (0.8)	-0.03 (0.63)	0.32 (0.54)	0.05 (0.92)	-0.17 (0.21)
	Interval 4 Slope Offset	**0.55 (0.01)**	**2.97 (0.07)**	1 (0.34)	**1.68 (0.02)**	0.26 (0.26)	0.76 (0.37)	0.89 (0.35)	**0.58 (0.05)**
	Interval5:SlopeInterval 5 Sl	**0.37 (<.01)**	0.61 (0.24)	0.62 (0.29)	**0.84 (<.01)**	**0.16 (0.01)**	0.01 (0.99)	-0.34 (0.46)	**0.51 (<.01)**
	Interval 6 Slope Offset	**0.22 (0.04)**	0.62 (0.18)	0 (1)	**0.7 (0.01)**	0.16 (0.23)	-0.45 (0.48)	-0.51 (0.43)	0.53 (0.16)
	Interval 7 Slope Offset					**0.35 (<.01)**	0.33 (0.65)	-0.71 (0.25)	0.51 (0.12)
JASO	**Calibration Intercept**	**2.81 (0.06)**	**243.07 (<.01)**	-10.8 (0.9)	**-30.01 (0.08)**	0.77 (0.58)	**74.68 (0.01)**	-28.12 (0.81)	-17.2 (0.15)
	Interval 2 Intercept offset	-99.82 (0.66)	-469.79 (0.14)	-58.03 (0.91)	62 (0.26)	11.03 (0.97)	-115.91 (0.58)	34.73 (0.96)	**113.08 (0.01)**
	Interval 3 Intercept offset	**6.9 (0.01)**	**-188.43 (0.03)**	97.56 (0.44)	**59.12 (0.05)**	**8.78 (<.01)**	42.83 (0.45)	26.43 (0.88)	**59.4 (0.01)**
	Interval 4 Intercept offset	2.27 (0.72)	**-326.03 (<.01)**	471.98 (0.16)	32.72 (0.59)	3.45 (0.52)	28.11 (0.84)	269.54 (0.57)	28.06 (0.39)
	Interval 5 Intercept offset	**7.34 (0.01)**	-123.61 (0.17)	117.57 (0.25)	**60.97 (0.05)**	3.68 (0.14)	74.82 (0.23)	234.72 (0.1)	**38.89 (0.05)**
	Interval 6 Intercept offset	-1.71 (0.62)	**-152.13 (0.09)**	150.67 (0.31)	23.83 (0.55)	-5.88 (0.67)	271.19 (0.25)	759.64 (0.27)	37.33 (0.86)
	Interval 7 Intercept offset					-0.29 (0.96)	59.62 (0.51)	174.72 (0.49)	-88.26 (0.12)
	Calibration Slope	**1.05 (<.01)**	0.34 (0.41)	**1.23 (<.01)**	**2.57 (<.01)**	**1.35 (<.01)**	**0.49 (0.05)**	**1.25 (<.01)**	**2.61 (<.01)**
	Interval 2 Slope Offset	9.8 (0.65)	9.77 (0.45)	2.78 (0.74)	**-1.82 (0.05)**	-0.14 (1)	3.02 (0.7)	0.94 (0.94)	**-2.14 (<.01)**
	Interval 3 Slope Offset	-0.27 (0.22)	-0.01 (0.99)	**-1.06 (0.04)**	**-1.54 (0.09)**	-0.21 (0.38)	-0.37 (0.61)	1.16 (0.11)	**-1.1 (0.07)**
	Interval 4 Slope Offset	-0.07 (0.9)	6.26 (0.18)	0.92 (0.91)	-1.12 (0.48)	-0.38 (0.4)	0.44 (0.89)	0.74 (0.95)	-1.22 (0.14)
	Interval5:SlopeInterval 5 Sl	**-0.34 (0.05)**	0.02 (0.98)	-0.22 (0.31)	**-1.71 (0.02)**	-0.21 (0.2)	0.54 (0.37)	0.07 (0.84)	**-1.09 (0.01)**
	Interval 6 Slope Offset	-0.2 (0.24)	-0.23 (0.67)	**-1.27 (0.09)**	**-1.56 (0.03)**	-0.08 (0.85)	-1.13 (0.26)	-3.22 (0.22)	-1.19 (0.48)
	Interval 7 Slope Offset					0.03 (0.9)	0.11 (0.9)	-0.52 (0.72)	0.94 (0.27)

Table 5: Linear model coefficients and P-values. Intercepts and intercept offsets are in units of mm (water) and kg km^{-2} (TSS). Coefficients significant at the P=0.1 level are in bold.

Season	Watershed	SR-LI	FW-LI	FW-SR
MAMJ	WS1	249.8 (.98)	1824.5 (.39)	1574.8 (.49)
MAMJ	WS2	521.0 (.89)	1080.6 (.61)	559.6 (.88)
MAMJ	WS3	858.9 (.50)	1043.7 (.36)	184.8 (.97)
JASO	WS1	-354.8 **(**.27**)**	224.9 (.59)	**579.7 (.04)**
JASO	WS2	-273.4 **(**.55**)**	457.8 (.20)	**731.2 (.02)**
JASO	WS3	-273.2 **(**.12**)**	162.1 (.47)	**435.4 (.01)**

Table 6: Results of Tukey's HSD test applied to seasonal yields by season and watershed. Values are the mean difference between statistical regression (SR), linear interpolation (LI), and flow-weighting (FW), with p-values in parentheses. Differences are presented in units of kg km-2 per season.

		WS1		WS2		WS3	
		Mean	**95%**	**Mean**	**95%**	**Mean**	**95%**
JASO	**Linear Interpolation**	179	455	208	539	135	526
	Flow-weighting	264	1192	361	1700	196	732
	Statistical Regression	94	189	141	320	69	168
MAMJ	**Linear Interpolation**	1117	4963	1074	3525	597	1773
	Flow-weighting	1661	7499	1418	4593	901	3046
	Statistical Regression	1176	5657	1202	4785	810	3120

Table 7 Mean and 95th percentile of monthly TSS discharge estimates [kg km^{-2}] for each watershed, by season and method.

	April LI	April FW	April SR	Oct. LI	Oct. FW	Oct. SR
Mean	7597	11883	7040	2124	3952	128
SD	299	544	89	182	381	2

Table 8 Sensitivity analysis results for April 2012 and October 1995. All units are in kg km^{-2}.

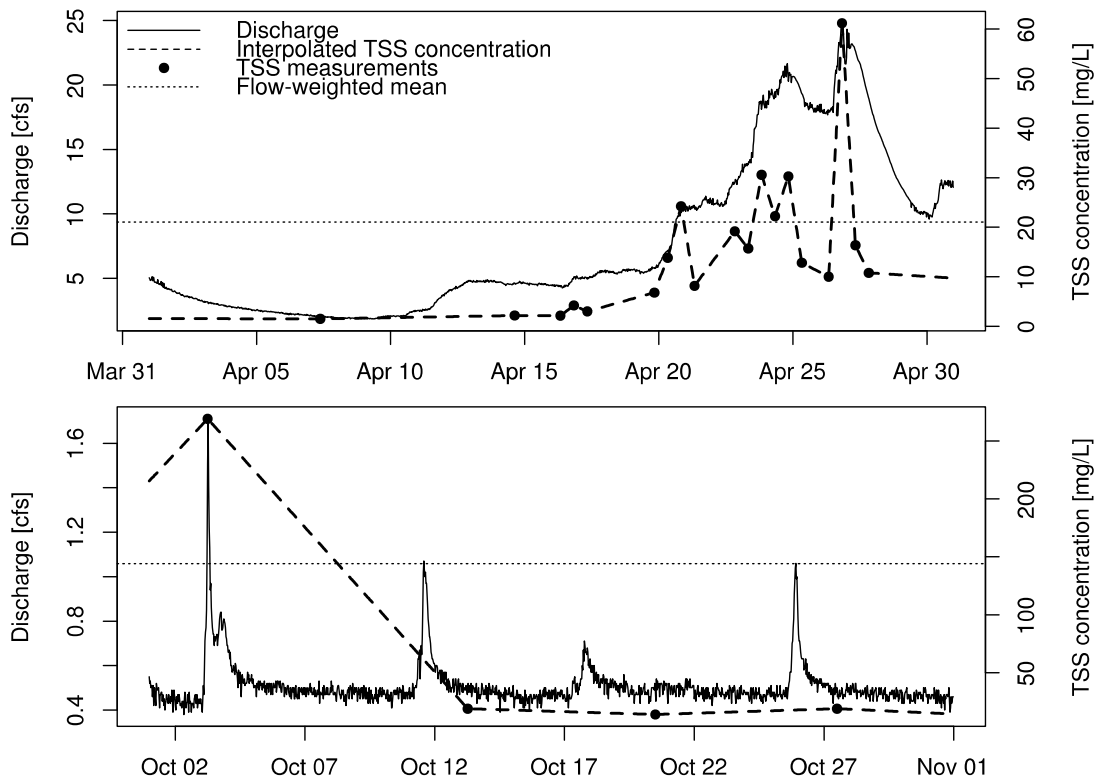

Figure 2 Hydrographs for April 2012 and October 1995, with TSS measurements, interpolation, and monthly flow-weighted mean. Flow weighted TSS yields: 6755 kg km^{-2} (Apr 2012) and 3959 kg km^{-2} (Oct 1995). Linear interpolation TSS yields: 4483 kg km^{-2} (Apr 2012) 2127 kg km^{-2} (Oct 1995).

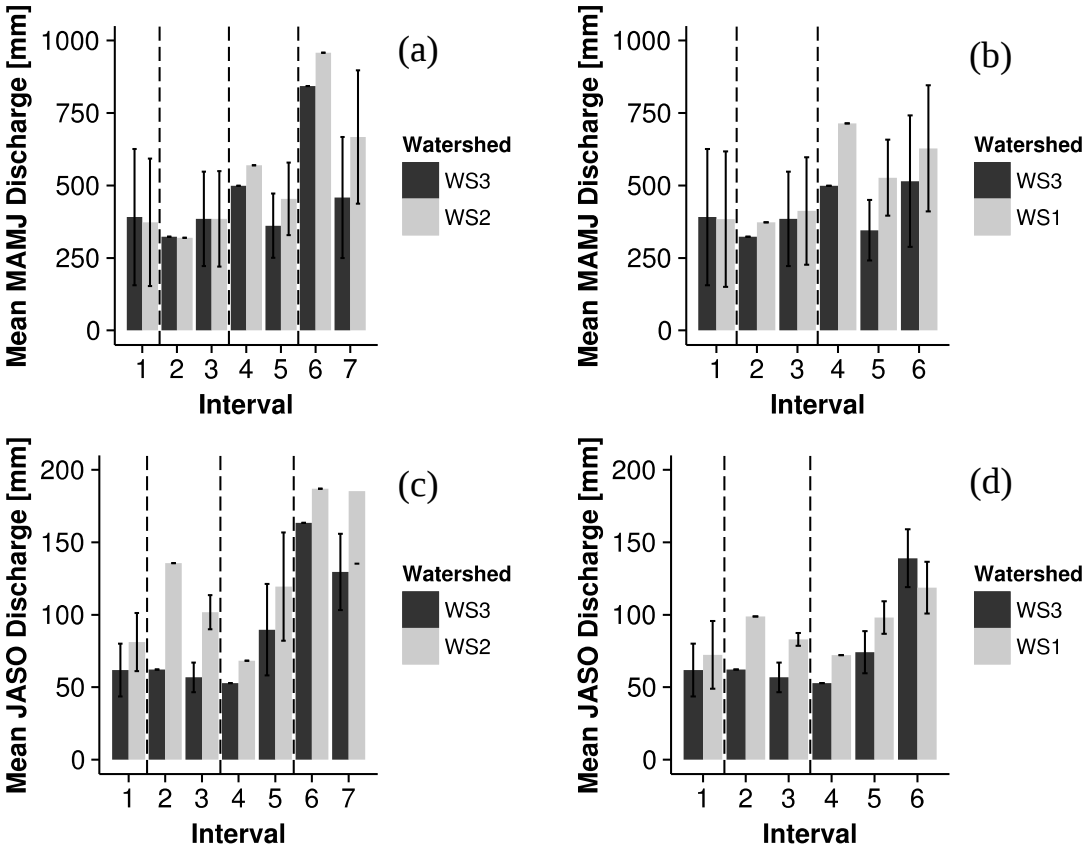

Figure 3 Mean seasonal water yields by interval and watershed. Vertical lines indicate road construction, initial thinning, and clearcut (WS2) and road construction and clearcut (WS1)

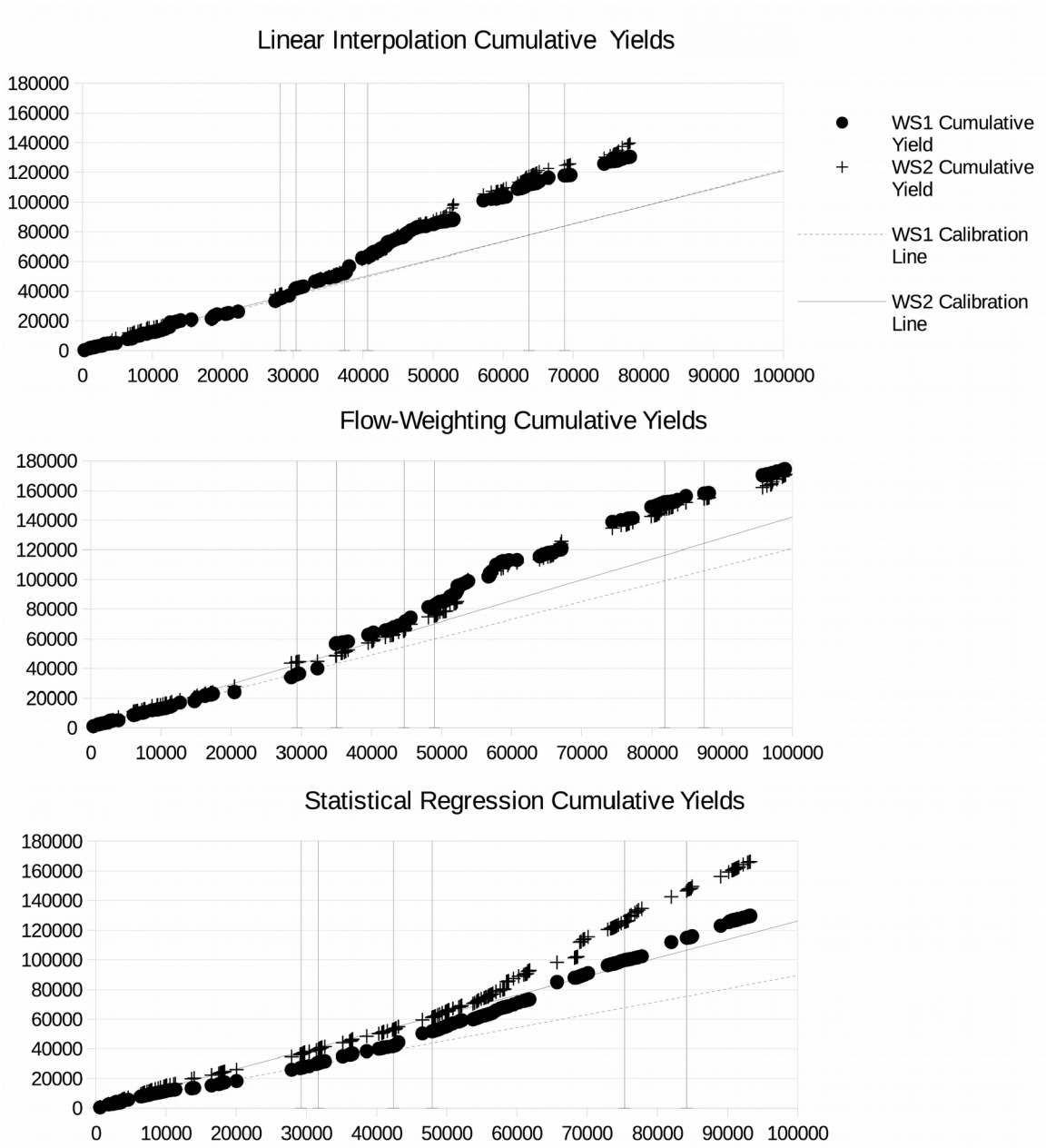

Figure 4 Cumulative yield [kg km^{-2}] double mass plots with WS1 and WS2 yields on the y-axis and WS3 yields on the x-axis. Vertical lines are placed at the transitions between treatment intervals.

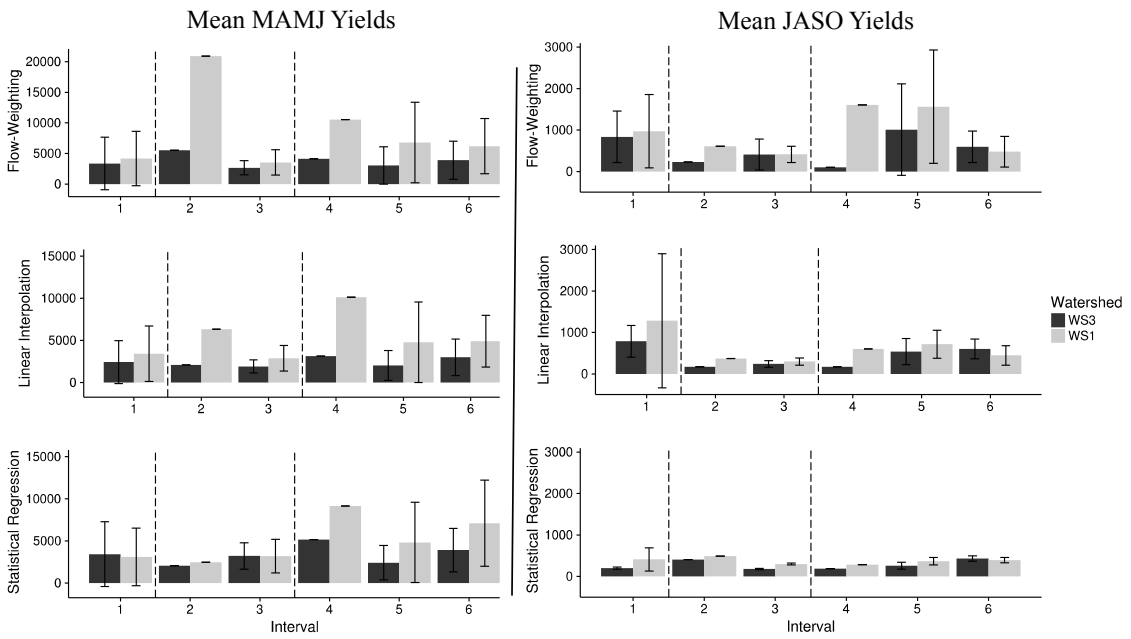

Figure 5 Mean Seasonal TSS yields for WS1 and WS3 [kg km^{-2}], with standard deviations.

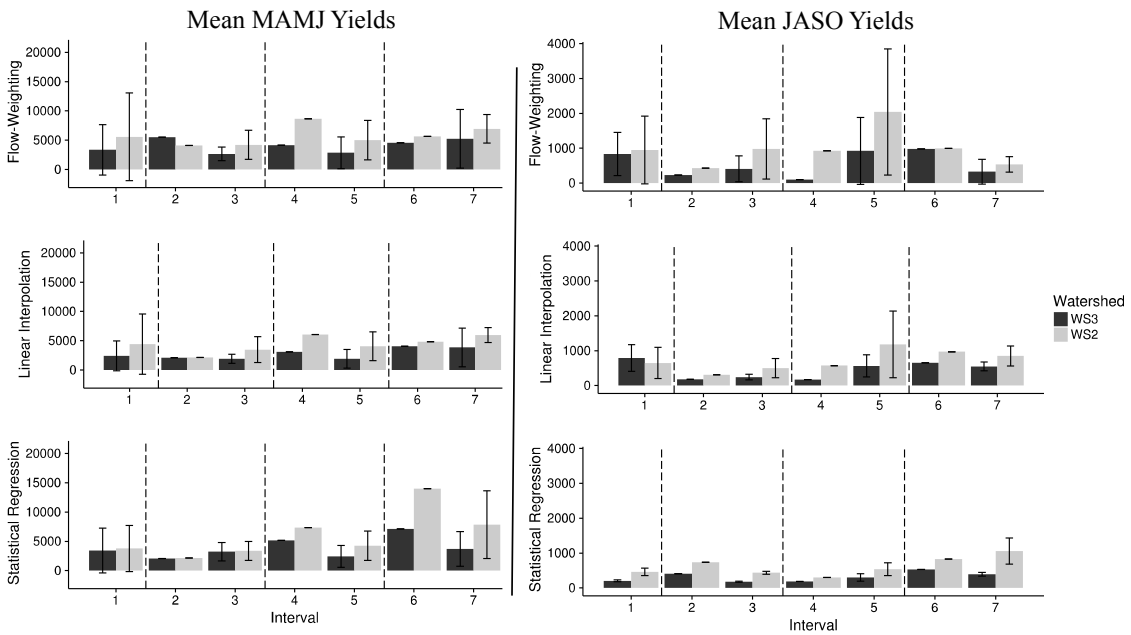

Figure 6 Mean Seasonal TSS yields for WS2 and WS3 [kg km^{-2}], with standard deviations.

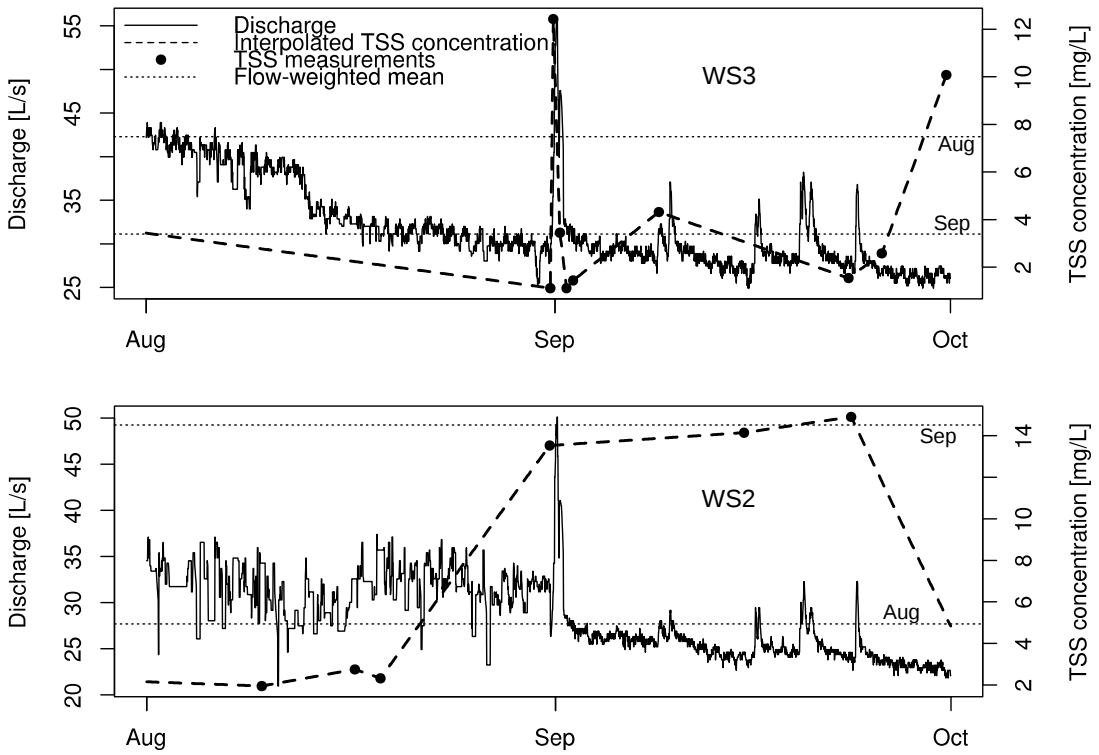

Figure 7 Hydrographs from WS2 and WS3 for August and September of 2010, with respective month's flow-weighted TSS estimates labeled.

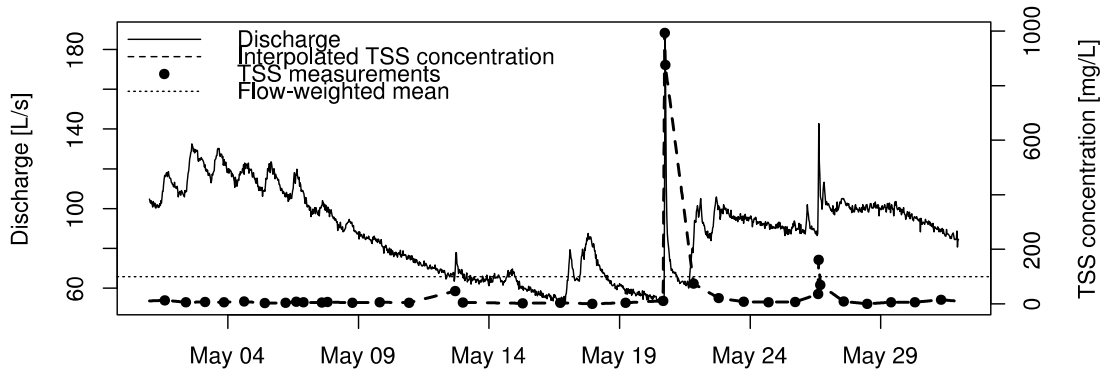

Figure 8WS1 hydrograph for May 1998

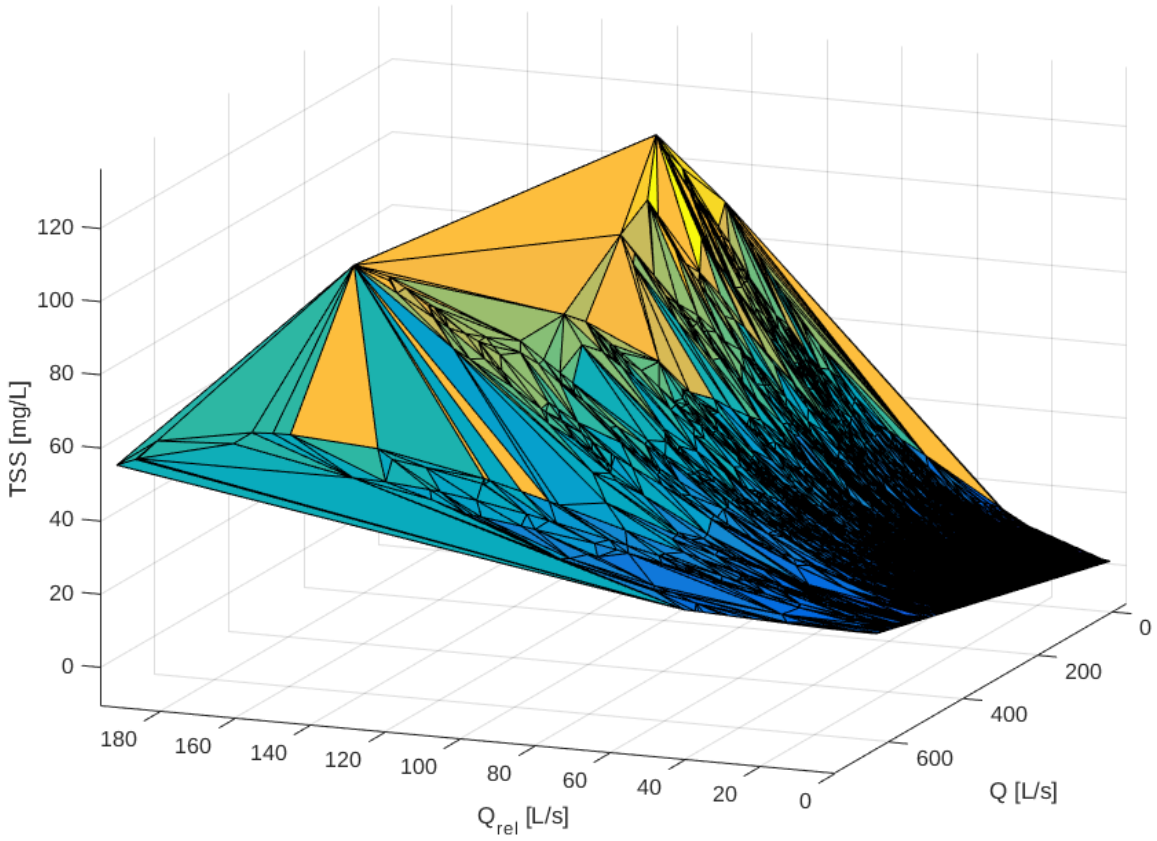

Figure 9 TSS statistical regression for MAMJ melt days at WS2

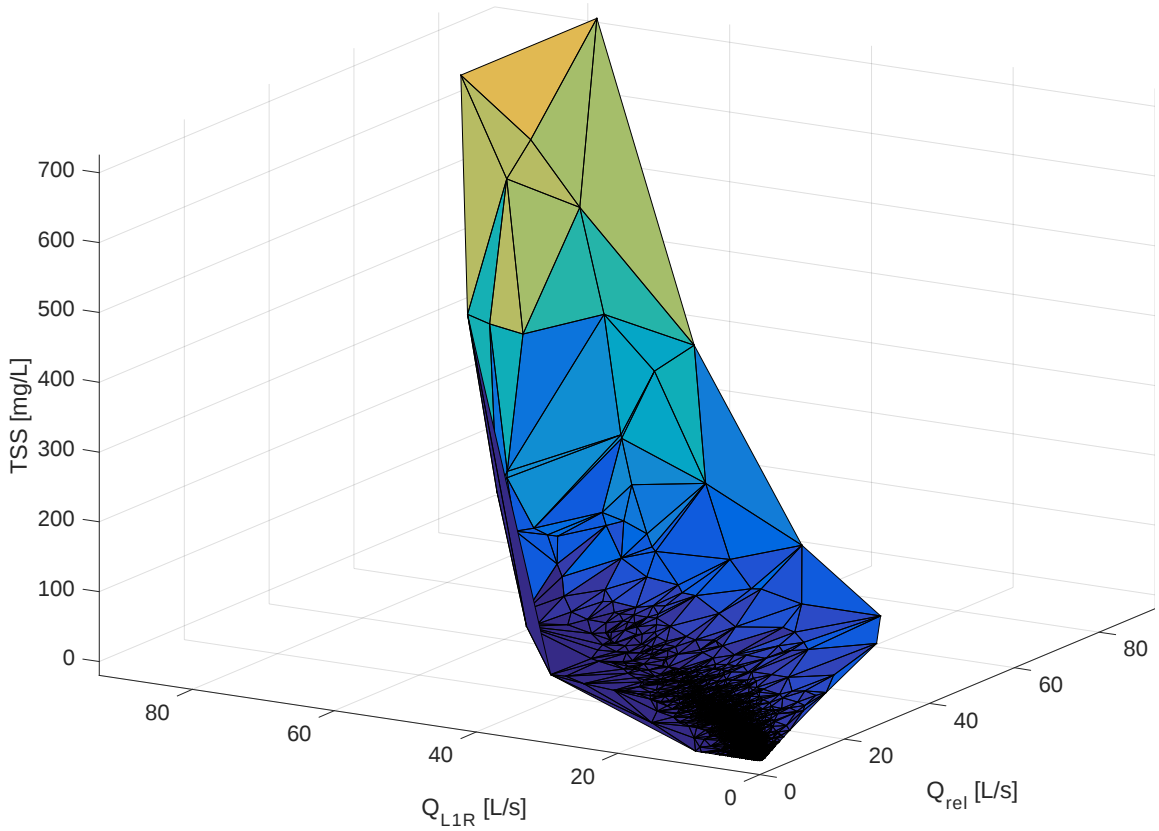

Figure 10 TSS statistical regression for JASO storms at WS3

LITERATURE CITED

Appling, A. P., M. C. Leon, and W. H. McDowell (2015), Reducing bias and quantifying uncertainty in watershed flux estimates: the R package loadflex, *Ecosphere*, *6*(12), art269, doi:10.1890/ES14-00517.1.

Baillie, B. R., K. J. Collier, and J. Nagels (2005), Effects of forest harvesting and woody debris removal on two Northland streams, New Zealand, *New Zeal. J. Mar. Freshw. Res.*, *39*(1), 1–15, doi:10.1080/00288330.2005.9517290.

Bathurst, J., and A. Iroume (2014), Quantitative Generalizations for Catchment Sediment Yield Following Plantation Logging, *Water Resour. Res.*, *16*, 2648, doi:10.1002/2014WR015711.Received.

Benaman, J., and C. a. Shoemaker (2005), An analysis of high-flow sediment event data for evaluating model performance, *Hydrol. Process.*, *19*(3), 605–620, doi:10.1002/hyp.5608.

Bilotta, G. S., and R. E. Brazier (2008), Understanding the influence of suspended solids on water quality and aquatic biota, *Water Res.*, *42*(12), 2849–2861, doi:10.1016/j.watres.2008.03.018.

Coats, R., F. J. Liu, and C. R. Goldman (2002), A Monte Carlo test of load calculation methods, Lake Tahoe basin, California-Nevada, *J. Am. Water Resour. Assoc.*, *38*(3), 719–730, doi:10.1111/j.1752-1688.2002.tb00992.x.

Droppo, I. G. (2001), Rethinking what constitutes suspended sediment, *Hydrol. Process.*, *15*(9), 1551–1564, doi:10.1002/hyp.228.

Droppo, I. G., K. Nackaerts, D. E. Walling, and N. Williams (2005), Can flocs and water stable soil aggregates be differentiated within fluvial systems?, *Catena*, *60*(1), 1–18, doi:10.1016/j.catena.2004.11.002.

Gravelle, J. a., G. Ice, T. E. Link, and D. L. Cook (2009), Nutrient concentration dynamics in an inland Pacific Northwest watershed before and after timber harvest, *For. Ecol. Manage.*, *257*(8), 1663–1675, doi:10.1016/j.foreco.2009.01.017.

Gray, J., and F. Simões (2008), Estimating Sediment Discharge, in *Sedimentation Engineering – Processes, Measurements, Modeling, and Practice, Manual 110*, edited by M. Garcia, pp. 1065–1086, Am. Soc. of Civ. Eng., Reston, VA.

Greer, M., S. Crow, A. Hicks, and G. Closs (2015), The effects of suspended sediment on brown trout (Salmo trutta) feeding and respiration after macrophyte control, *New Zeal. J. Mar. Freshw. Res.*, *49*(2), 278–285, doi:10.1080/00288330.2015.1013140.

Hubbart, J. A., T. E. Link, J. A. Gravelle, and W. J. Elliot (2007), Timber harvest impacts on water yield in the continental/maritime hydroclimatic region of the United States, *For. Sci.*, *53*(2), 169–180.

Karwan, D. L., J. A. Gravelle, and J. A. Hubbart (2007), Effects of timber harvest on suspended sediment loads in Mica Creek, Idaho, *For. Sci.*, *53*(2), 181–188.

Loftis, J. C., L. H. MacDonald, S. Streett, H. K. Iyer, and K. Bunte (2001), Detecting cumulative watershed effects: The statistical power of pairing, *J. Hydrol.*, *251*(1-2), 49–64, doi:10.1016/S0022-1694(01)00431-0.

Lowe, M., M. Morrison, and R. Taylor (2015), Harmful effects of sediment-induced turbidity on juvenile fish in estuaries, *Mar. Ecol. Prog. Ser.*, *539*, 241–254, doi:10.3354/meps11496.

MacDonald, L., and J. Stednick (2003), *Forests and Water : A State-of-the-Art Review for Colorado*.

Megahan, W. F., J. G. King, and K. a Seyedbagheri (1995), Hydrologic and erosional responses of a granitic watershed to helicopter logging and broadcast burning, *For. Sci.*, *41*(4), 777–795.

Narula, S. C. (1979), Orthogonal Polynomial Regression, *Int. Stat. Rev.*, *47*, 31–36.

Nistor, C. J., and M. Church (2005), Suspended sediment transport regime in a debris-flow gully on Vancouver Island, British Columbia, *Hydrol. Process.*, *19*(4), 861–885, doi:10.1002/hyp.5549.

Owens, P. N. et al. (2005), Fine-grained sediment in river systems: environmental significance and management issues, *River Res. Appl.*, *21*(7), 693–717, doi:10.1002/rra.878.

Quilbé, R., A. N. Rousseau, M. Duchemin, A. Poulin, G. Gangbazo, and J. P. Villeneuve (2006), Selecting a calculation method to estimate sediment and nutrient loads in streams: Application to the Beaurivage River (Québec, Canada), *J. Hydrol.*, *326*(1-4), 295–310, doi:10.1016/j.jhydrol.2005.11.008.

Raymond, S., A. Mailhot, G. Talbot, P. Gagnon, A. N. Rousseau, and F. Moatar (2014), Load estimation method using distributions with covariates: A comparison with

commonly used estimation methods, *J. Am. Water Resour. Assoc.*, *50*(3), 791–804, doi:10.1111/jawr.12147.

Redding, J. M., C. B. Schreck, and F. H. Everest (1987), Physiological Effects on Coho Salmon and Steelhead of Exposure to Suspended Solids, *Trans. Am. Fish. Soc.*, *116*(5), 737–744, doi:10.1577/1548-8659(1987)116<737:PEOCSA>2.0.CO;2.

Runkel, R. L., C. G. Crawford, and T. a Cohn (2004), Load Estimator (LOADEST): A FORTRAN program for estimating constituent loads in streams and rivers, *Tech. Methods. U.S. Geol. Surv. U.S. Dep. Inter.*, *4*, 69.

Ryan, P. a. (1991), Environmental effects of sediment on New Zealand streams: A review, *New Zeal. J. Mar. Freshw. Res.*, *25*(February), 207–221, doi:10.1080/00288330.1991.9516472.

Smart, T. S., D. J. Hirst, and D. a. Elston (1999), Methods for estimation loads transported by rivers, *Hydrol. Earth Syst. Sci.*, *3*(2), 295–303, doi:10.5194/hess-3-295-1999.

Underwood, J. W., C. E. Renshaw, F. J. Magilligan, W. B. Dade, and J. D. Landis (2015), Joint isotopic mass balance : a novel approach to quantifying channel bed to channel margins sediment transfer during storm events, , doi:10.1002/esp.3734.

Vericat, D., and R. J. Batalla (2006), Sediment transport in a large impounded river: The lower Ebro, NE Iberian Peninsula, *Geomorphology*, *79*(1-2), 72–92, doi:10.1016/j.geomorph.2005.09.017.

Wotton, R. S. (2007), Do benthic biologists pay enough attention to aggregates formed in the water column of streams and rivers?, *J. North Am. Benthol. Soc.*, *26*(1), 1–11.